THE JOURNAL OF BIOLOGICAL CHEMISTRY
Vol. 276, No. 14, Issue of April 6, pp. 11189–11198, 2001

Printed in U.S.A.

Myomegalin Is a Novel Protein of the Golgi/Centrosome That Interacts with a Cyclic Nucleotide Phosphodiesterase*

Received for publication, July 21, 2000, and in revised form, December 6, 2000
Published, JBC Papers in Press, December 27, 2000, DOI 10.1074/jbc.M006546200

Ignacio Verde‡§, Gudrun Pahlke‡§, Michele Salanova‡, Gu Zhang‡, Sonya Wang‡, Dario Coletti‡, James Onuffer¶, S.-L. Catherine Jin‡, and Marco Conti‡‖

From the ‡Division of Reproductive Biology, Department of Gynecology and Obstetrics, Stanford University School of Medicine, Stanford, California 94305-5317 and the ¶Department of Immunology, Berlex Biosciences, Richmond, California 94804-0099

Subcellular targeting of the components of the cAMP-dependent pathway is thought to be essential for intracellular signaling. Here we have identified a novel protein, named myomegalin, that interacts with the cyclic nucleotide phosphodiesterase PDE4D, thereby targeting it to particulate structures. Myomegalin is a large 2,324-amino acid protein mostly composed of α-helical and coiled-coil structures, with domains shared with microtubule-associated proteins, and a leucine zipper identical to that found in the *Drosophila* centrosomin. Transcripts of 7.5–8 kilobases were present in most tissues, whereas a short mRNA of 2.4 kilobases was detected only in rat testis. A third splicing variant was expressed predominantly in rat heart. Antibodies against the deduced sequence recognized particulate myomegalin proteins of 62 kDa in testis and 230–250 kDa in heart and skeletal muscle. Immunocytochemistry and transfection studies demonstrate colocalization of PDE4D and myomegalin in the Golgi/centrosomal area of cultured cells, and in sarcomeric structures of skeletal muscle. Myomegalin expressed in COS-7 cells coimmunoprecipitated with PDE4D3 and sequestered it to particulate structures. These findings indicate that myomegalin is a novel protein that functions as an anchor to localize components of the cAMP-dependent pathway to the Golgi/centrosomal region of the cell.

Only in recent years has it been realized that the components of the signal transduction machinery are organized in macromolecular complexes located in close proximity to the plasma membrane or in discrete subcellular structures. These complexes are assembled by scaffold proteins often devoid of enzymatic activity and for the sole function of bringing together different signaling molecules (1, 2). These signaling/scaffold protein complexes are necessary and often indispensable for signaling, as disruption or blocking the formation of these complexes decreases the efficiency of signaling or negates it altogether.

Even though cAMP is a diffusible second messenger, the enzymes involved in this signaling pathway are targeted to different subcellular compartments. With few exceptions, adenylyl cyclases are plasma membrane-associated proteins, and protein kinase A (PKA),[1] one of the effectors of cAMP signaling, is anchored to discrete structures within the cell via regulatory subunit interaction with A kinase anchoring proteins (AKAPs) (3, 4). Several different AKAPs that function as scaffold proteins have been characterized. For instance, AKAP79 is part of a multicomplex, which, in addition to the PKA regulatory subunit RII, includes protein kinase C and the phosphatase PP2B/calcineurin (5). Disruption of the PKA interaction with AKAPs abolishes the cAMP-dependent regulation of ion channels (6, 7). PKA regulatory subunits have also been localized in the centrosome in culture cells (8), and in cells of the central nervous system (9), thus opening the possibility that microenvironments of cAMP signaling may be necessary for intracellular trafficking and organelle movements during cell replication.

Cyclic nucleotide phosphodiesterases, the enzymes that degrade and inactivate cAMP, may play an important role in signaling compartmentalization by controlling cAMP diffusion to reach the PKA isoenzymes anchored to different organelles. Of the wide array of PDE isoforms present in a cell (10–13), several are recovered in the particulate fraction of the homogenate and have been immunolocalized to different cellular compartments. We and others have shown that variants derived from the PDE4D gene are particulate or soluble, depending on the amino terminus present in the protein (14–16), and are located in different subcellular compartments as shown by immunofluorescence studies. In FRTL-5 thyroid cells, two variants (PDE4D3 and PDE4D4) with long amino termini are recovered in the particulate fraction, and are localized in a perinuclear region corresponding to centrosomal inner/Golgi structures, as well as to the membrane cortical region (16). Conversely, a third variant (PDE4D2), the expression of which is cAMP-dependent, is recovered mostly in the soluble fraction and its induction by cAMP is associated with diffuse immunofluorescent signals in these cells (16). Localization of PDE4D in discrete subcellular structures has also been demonstrated in macrophages (17). These findings open the possibility that the subcellular localization of PDE4D is finely controlled and this localization may be dynamically regulated during cAMP signaling.

* This work was supported by National Institutes of Health Grant RO1-HD20788 and by a gift from Berlex (to G. P.). The costs of publication of this article were defrayed in part by the payment of page charges. This article must therefore be hereby marked "*advertisement*" in accordance with 18 U.S.C. Section 1734 solely to indicate this fact. *The nucleotide sequence(s) reported in this paper has been submitted to the GenBank™/EBI Data Bank with accession number(s) AF139185.*

§ These authors contributed equally to this study.
‖ To whom correspondence should be addressed. Tel.: 650-725-2452; Fax: 650-725-7102; E-mail: marco.conti@stanford.edu.

[1] The abbreviations used are: PKA, protein kinase A; AKAP, A kinase anchoring protein; PDE, phosphodiesterase; kb, kilobase pair(s); bp, base pair(s); ORF, open reading frame; RT, reverse transcriptase; PCR, polymerase chain reaction; AD, activation domain; 3-AT, 3-amino-1,2,4,-triazole; PAGE, polyacrylamide gel electrophoresis; SD, selection medium; PBS, phosphate-buffered saline; TBS-T, Tris-buffered saline with Tween 20; aa, amino acid(s); MOPS, 4-morpholinepropanesulfonic acid; RIPA, radioimmune precipitation assay.

To understand the mechanism of PDE4 subcellular targeting, we sought to identify proteins that interact with these PDE4D variants and to anchor them to different organelles. Here we describe the properties of a novel protein named myomegalin, which is a major component of skeletal and cardiac muscle but is expressed at low levels in all cells studied. Although in nonmuscle cells it is targeted to the Golgi/centrosomal region, myomegalin localizes in the sarcomeres in heart and skeletal muscle. This protein colocalizes with PDE4D in the cells and tissue studied.

EXPERIMENTAL PROCEDURES

Yeast Strains and Growth Conditions—The yeast strains of *Saccharomyces cerevisiae* (Y190, HF7c, Y187), cloning vectors, and the activating domain (AD) rat brain cDNA library used for the yeast two-hybrid screening (Matchmaker I and II) as well as the λgt11 cDNA libraries (from rat brain and rat skeletal muscle) were obtained from CLONTECH (Palo Alto, CA), yeast media from Difco (Detroit, MI), and amino acids and 3-amino-1,2,4,-triazole (3-AT) from Sigma. Restriction enzymes were purchased from Roche Molecular Biochemicals, DNA modifying enzymes and PCR reagents from Life Technologies, Inc. or Stratagene (La Jolla, CA).

The yeast strain Y190 of *S. cerevisiae* was used as host for the yeast two-hybrid screening, whereas HF7c and Y187 were used for mating experiments. Yeast transformation was performed using the lithium acetate method according to Gietz *et al.* (47). Single transformants were spread on selection medium (SD medium) lacking Leu or Trp. Cotransformants of strain Y190 were propagated on SD medium containing Ade (10 mg/ml) and 50 mM 3-AT. Single transformants of Y187 were grown on SD medium lacking Trp. The yeast strain HF7c was transformed with Gal4 activation domain expressing His+Z+ clones from the library screen. Transformants were propagated on SD/−Leu.

Yeast Two-hybrid Screening of a Brain cDNA Library—The yeast strain Y190 was used to screen a rat brain Gal4/AD library to identify genes encoding proteins that interact with ratPDE4D3. The amino terminus (aa 1–133) of PDE4D3 as well as a truncated form of ratPDE4D3 that included the autoinhibitory (UCR2), catalytic, and COOH-terminal domain (aa 134–end of rPDE4D3) were used as a bait. The cDNA corresponding to the truncated PDE (base 400–2018 of the PDE4D3 ORF, accession no. U09457) was amplified by PCR using the full-length ratPDE4D3 cDNA as a template. The following primers with incorporated restriction sites were used: GUPA4, *Eco*RI 5′-CGGAATTCGAGGAGGCCTACCAGAAAC-3′; and GUPA3, 5′-TGAGTCGACTACGTGTCAGGACAACAATCGTC-3′ *Sal*I. The PCR product was subcloned into the *Eco*RI/*Sal*I site of pGBT9 downstream from the Gal4 DNA binding domain (plasmid pGBT9/1.6). Amplifications were performed in the presence of recombinant *Pfu* polymerase at a low cycle number to ensure high fidelity amplification. The amplified fragment was sequenced in its entire length to confirm the correct reading frame and sequence. Sequencing was performed by Stanford University facilities using the ABI PRISM Dye Terminator Cycle Sequencing Ready Reaction kit with AmpliTaq DNA polymerase, FS (PerkinElmer Life Sciences). Further truncations of ratPDE4D3 were obtained as reported previously (18) to identify the PDE domain responsible for the interaction with positive AD/library clones. These included PDEtruA (aa 164–end), PDEtruB (aa 179–end), and PDEtruC (214–end). The construction of the plasmid containing the amino terminus of PDE4D3 (0.4) has been described previously (18). Under the experimental conditions used, the full-length PDE4D3 (93 kDa) did not express well as a fusion protein in yeast nuclei.

A portion of the AD/cDNA plasmid library was amplified once to obtain sufficient plasmid DNA for screening. The plasmid DNAs of bait and library (concentration ratio 2:1) were simultaneously transformed into Y190 cells on a large scale basis according to the manufacturer's protocol. Protein expression in Y190 was induced on SD/Ade, 50 mM 3-AT (6.7 g/liter yeast nitrogen base without amino acids, pH 5.8; 18 g/liter agar, 10 mg/liter adenine, 2% dextrose, and 50 mM 3-amino-1,2,4-triazole). Transcriptional autoactivation of the pGBT9/1.6 was monitored by single and cotransformation with control plasmids containing the Gal4 transcriptional activation domain alone (pGAD10) or with other in frame cDNAs such as the SV40 large T-antigene (pTD1) and pGAD10/1.6. No background for β-galactosidase activity was detected after overnight incubation at 30 °C.

After 7–19 days of incubation at 30 °C, the colonies growing on His+ plates were counted and patched onto fresh SD/Ade, 50 mM 3-AT, together with controls. The first group of patched His+ clones was checked again for positive growth 5 days after incubation. At that stage, a β-galactosidase filter lift assay was carried out to detect positive clones. Each His+Z+ clone was restreaked on SD/Ade, 50 mM 3-AT medium to generate single clones. Single colonies were reassayed for β-galactosidase activity. The clones obtained by screening with the amino terminus of PDE4D3 will be reported elsewhere.

To isolate Leu+Trp+ yeast segregants with only the AD/library plasmid, His+Z+ transformants were cultured in YPD medium overnight at 30 °C. An aliquot of the sample was spread on SD/−Leu and incubated for 3 days. Colonies were replica-plated on SD/−Leu only and on SD/−Leu,−Trp plates. Colonies growing on SD/−Leu plates (+Trp) but not on SD/−Leu,−Trp (−Trp) carry the AD/library plasmid; however, the plasmid containing the bait had been lost. These Trp auxotrophs were reassayed for β-galactosidase activity. Negative clones were saved. Plasmid DNA was isolated from Trp auxotrophs according to the manufacturer's protocol and was used for transformation into *E. coli* strain HB101 using electroporation (Genepulser, Bio-Rad).

To confirm the interaction of the isolated clones with the bait, yeast strain Y190 and HF7c were retransformed with bait and AD/library plasmid and tested for yeast mating and for β-galactosidase expression. To measure the β-galactosidase activity in transformants, the colony lift filter assay was done according to the manufacturer's protocol (CLONTECH). Blue colonies were developed after incubation overnight at 30 °C.

Yeast Mating—Yeast strain Y187 was transformed with pGBT9 and pGBT9/1.6 and selected for Trp+ transformants. Yeast strain HF7c was single transformed with pGAD10, pGAD10/library positive clones. Transformants were propagated on SD/−Leu. Individual positive colonies for Trp and Leu were streaked separately on the corresponding SD medium and grown for 3–4 days at 30 °C. The different transformants of Trp+ and Leu+ were replica-plated in a grid pattern on YPD plates and incubated overnight at 30 °C. Colonies of diploid cells were replica-plated on SD medium lacking Leu, Trp, and His. After ~6 days, His+ colonies were counted and LacZ expression was detected using the β-galactosidase assay.

Cloning by Library Screening—To obtain the complete sequence of the PDE4D3-interacting protein myomegalin, the PBP46 cDNA isolated from the yeast library screening was used as a probe to screen rat brain and skeletal muscle λgt11 libraries (CLONTECH). Three of the more than 50 clones retrieved were sequenced, and the overlap with PBP46 was established by multiple sequence alignment. Because the potential initiation codon was absent in all three clones, oligonucleotides corresponding to the 5′ end of the new open reading frame were designed and used for further screening of the same library. This procedure was repeated four times until a clone containing in-frame stop codons upstream from the putative initiation codon was retrieved. Overlapping cDNAs were used to reconstruct the entire open reading frame of myomegalin. Melds were confirmed by at least two overlapping clones. Three of the clones retrieved contained 5′ ends that could not be aligned with the reconstructed open reading frame. Whether these clones encompass splicing junctions or are cloning artifacts was not further investigated.

Northern Blot Analysis—Two different DNA probes (probe 1, 1000 bp; probe 2, 665 bp) derived from the ORF of myomegalin were labeled with [α-^{32}P]dCTP by the random primer procedure (Life Technologies, Inc.). The labeled probes were purified using Quick Spin G-25 Sephadex columns (Roche Molecular Biochemicals) and used to hybridize a rat multiple tissue Northern blot (CLONTECH). Hybridization and washing procedures were carried out according to the manufacturer's protocol.

RT-PCR Analysis—Poly(A$^+$) mRNA was isolated from rat heart and skeletal muscle using the QuickPrep Micro mRNA purification kit (Amersham Pharmacia Biotech). First strand cDNA was prepared from mRNA with random hexanucleotide primers (20 pmol/μg of RNA) using murine reverse transcriptase and the conditions recommended by the manufacturer's protocol (Amersham Pharmacia Biotech). The cDNA obtained was amplified with the following oligonucleotide primers designed against different regions of myomegalin: MYO1-MYO2, forward primer (5′-GTGGAGAGCCTGAAAACGAGAG-3′, corresponding to bases 163–183 (aa 55–61)) and reverse primer (5′-AGTCGTCTCAGAAGCAAGATACGA-3′, corresponding to bases 830–844 (aa 274–282); predicted fragment, size 682 bp); MYO3-MYO4, forward primer (5′-GAAGCTAGCTCTCCCCGCTACA-3′, corresponding to bases 5266–5287 (aa 1756–1764)) and reverse primer (5′-CTACGAGTCCCTCTACGAAAAT-3′, corresponding to bases 5987–6009 (aa 1995–2003; predicted fragment size, 743 bp)); KIA1-MYO2, forward primer (5′-CTGTGGAATCTTTGGATGCAAGCGT-3′, bp 1379–1403 of KIAA0477) and reverse primer (5′-AGTCGTCTCAGAAGCAAGATACGA-3′, frag-

ment size, 587 bp). Thirty cycles of PCR amplification were usually used (60 s at 94 °C, 60 s at 50 °C, and 2 min at 72 °C) and a final elongation (10 min at 72 °C). The PCR products were separated on 1% agarose gel containing 0.01% ethidium bromide and photographed under UV irradiation at 320 nm.

Antibody Generation—The peptide PBP4 (FASGHGRHVIGHVDDY-DALQQQI) was conjugated to keyhole limpet hemocyanin for immunizations in rabbits. The immunizations and bleeds were performed at Strategic BioSolutions, Inc. (Ramona, CA). For affinity purification, the PBP4 peptide was immobilized to 3 M Emphaze™ Biosupport Medium AB 1 using the Ultralink™ immobilized carboxy kit from Pierce. The PBP4-specific IgG was eluted from the column by sequential washes at low pH (ImmunoPure IgG elution buffer, Pierce) and at high pH (0.1 M triethylamine, pH 11.5). The antibodies were buffer exchanged to PBS and concentrated to 1 mg/ml using an Ultrafree-15 Biomax-30 centrifugal filter device (Millipore Corp., Bedford, MA).

Western Blot Analysis—Tissues or cells were homogenized in a Dounce homogenizer using a hypotonic buffer consisting of 20 mM Tris, pH 8.0, 1 mM EDTA, 0.2 mM EGTA, 50 mM NaF, 10 mM sodium pyrophosphate, 50 mM benzamidine, 0.5 μg/m leupeptin, 0.7 μg/ml pepstatin, 4 μg/ml aprotinin, 10 μg/ml soybean trypsin inhibitor, 1 μM microcystine, and 1 μg/ml phenylmethylsulfonyl fluoride (homogenization buffer). After homogenization the extract was centrifuged for 40 min at 14,000 $\times$ *g* to separate soluble and particulate fractions. Both fractions were diluted in 1$\times$ sample buffer (62.5 mM Tris, pH 6.8, 10% glycerol, 2% (w/v) SDS, 0.7 mM β-mercaptoethanol, and 0.0025% (w/v) bromphenol blue), boiled for 5 min, and subjected to electrophoresis on 8% SDS-polyacrylamide gel. The proteins were then blotted onto an Immobilon membrane (Bio-Rad), followed by blocking of the membrane in TBS-T (20 mM Tris-HCl, pH 7.6, 14 mM NaCl, 0.1% Tween 20) containing 0.1% (w/v) nonfat milk. After several washes, the membrane was incubated with the primary antibody (M3S1, PBP4 antiserum, or anti-flag tag antibody) in TBS-T for 60 min, then washed with TBS-T followed by another 1-h incubation with peroxidase-linked anti-rabbit or anti-mouse IgG. After several washes with TBS-T, the membrane was incubated with the ECL detection reagent (Amersham Pharmacia Biotech) and exposed to XAR-5 x-ray film for 5–120 s (Eastman Kodak Co.) to detect the peroxidase-conjugated secondary antibodies.

Freshly excised skeletal and heart tissue was frozen in liquid nitrogen. After pulverization, the tissue was extracted with buffer containing 5 mM EGTA, 7 mM ATP, 130 mM propionic acid, 5 mM imidazole, 10 mM MOPS, pH 7.2, and a mixture of protease inhibitors, following the method of Brandt *et al.* (20). After homogenization with all glass homogenizer, the samples were centrifuged at 100,000 $\times$ *g*. The pellets were extracted with 1$\times$ sample buffer and centrifuged at 14,000 $\times$ *g* to remove particulate material. After dilution in sample buffer, supernatants and pellets were fractionated by SDS-PAGE as above.

Transfection and Immunofluorescence Localization—The truncated myomegalin (63 kDa) was tagged with flag epitope (DYKDDDDK) at its NH_2 terminus by transferring the insert PBP46 to the *Bam*HI/*Bgl*II of a modified vector (gift of Dr. Louis Naumovsky, Stanford University, Stanford, CA) derived from pCEP4 (Invitrogen Corp., Carlsbad, CA). The construct was transfected in COS-7 cells using the calcium phosphate method (19). Cells were grown in Eagle's medium (Life Technologies) for 48 h, fixed with ethanol-acetone solution (1:1) for 10 min, preincubated with PBS containing 0.1% bovine serum albumin for 20 min, and then incubated with specific primary antibodies in PBS for 1 h. Rabbit polyclonal PBP4 antibody was used at 1:100 dilution, anti-flag at 1:80, CTR433 (median Golgi marker) (21) at 1:10, CTR453 (centrosomal marker) (22) at 1:500, and M3S1 at 1:50. After the cells were washed with PBS three times, fluorescent fluorescein isothiocyanate- or rhodamine-conjugated secondary antibodies (1:100 dilution; Vector Laboratories, Inc., Burlingame, CA) were then added to the cells. The expressed proteins were localized using fluorescence microscopy after mounting the samples with Vectashield mounting medium (Vector Laboratories, Inc.). Tissue immunofluorescence localization was performed according to previously published methods (23).

PDE Assay—PDE activity was measured with 1 μM cAMP as substrate according to the method of Thompson and Appleman (24) with minor modification (16). Protein concentrations of the samples were measured according to the method of Bradford (25).

RESULTS

Isolation of Clones Coding for Proteins That Interact with PDE4D in the Yeast Two-hybrid Screen—A yeast two-hybrid screening of a rat brain library with baits corresponding to amino acids 1–133 and 134–end of PDE4D3 (see Fig. 1) yielded several clones that interacted strongly with the PDE in both the β-galactosidase and yeast growth assays. Of these positive clones, one (PBP46) was further characterized because the sequence of this cDNA demonstrated only weak similarity with known sequences. The interaction with the PDE was evident whether the cDNA was fused to the activation or the DNA binding domain, and when either a growth or β-galactosidase assay was used (Fig. 1). Analysis using constructs containing the different PDE4D domains indicated that PBP46 interacted with the amino terminus of PDE4D in a region that corresponds to the upstream conserved region 2 (UCR2) of PDE4 (aa 134–164 of PDE4D3) (Fig. 1). This conclusion is based on the observation that constructs encoding aa 1–133 (0.4), aa 164–end (TruA), 179–end (TruB), and 214–end (TruC) of PDE4D3 (Fig. 1) did not interact with PBP46. This PDE domain is upstream from an autoinhibitory domain that controls the catalytic activity of the enzyme (18).

Cloning of the Full-length cDNA Coding for Myomegalin—Northern blot analysis with mRNAs from different rat tissues indicated that PBP46 cDNA corresponds to a gene that is expressed at a high level in skeletal muscle and heart (see below). A rat skeletal muscle λgt11 cDNA library was therefore repeatedly screened using the PBP46 cDNA as a probe. To obtain the entire ORF, the library was screened four times and 18 overlapping clones were characterized. A meld of these clones indicated the presence of an uninterrupted ORF of 6975 bp, which encodes a protein of 2324 amino acids with a calculated molecular mass of 262 kDa (Fig. 2). An additional 1000 bp of 3′-UTR and more than 500 bp of 5′-UTR are consistent with the 7.5–8-kb transcript detected by Northern blot analysis (see below). In view of the high level of expression in muscle cells and the large size of the encoded protein, this new gene was termed myomegalin (*mmg,* accession no. AF139185).

Myomegalin Structure—A computer-assisted prediction of the secondary structure of myomegalin indicated that this protein is mostly composed of coiled-coil and α-helical domains (Fig. 2*A*) with 20% identity to myosin heavy chains, even though no sequences similar to the ATP binding domain of the myosin heavy chain could be identified. The full-length protein contains a putative leucine zipper at the amino terminus between residues 8 and 31 and an uncharged region rich in proline close to the COOH-terminal region (Fig. 2, *A* and *B*). BLAST search comparison showed that the first domain is almost identical to the first leucine zipper of *Drosophila* centrosomin, a protein localized in the centrosome of *Drosophila melanogaster* (26). In addition, a domain between amino acids 769 and 784 is homologous to a domain of dynactin that is responsible for the binding to the actin-like protein centractin/ARP1. Dynactin and centractin are part of the complex implicated in vesicle transport and the interaction with the microtubules in mammalian cells (27). Finally, myomegalin contains a helix-loop-helix domain between amino acids 1079 and 1094. This domain is homologous with regions found in human CLIP-170 (cytoplasmic linker protein) and rat DAP-150 (dynein associated polypeptide) (Fig. 2*A*). CLIP-170 is a protein that binds microtubules and is implicated in the process of endocytosis and organelle transport in mammalians (28). The function of DAP-150 is still largely unknown (29). The myomegalin domains included in the testis variant (corresponding to the PBP46 clone, see below) contains mostly α-helices and two coil-coil regions, as indicated in Fig. 2. The presence of coil-coil regions and absence of putative transmembrane domains are consistent with recovery of expressed PBP46, a truncated myomegalin, in particulate fractions of transfected cells, and its resistance to solubilization with nonionic detergents alone.

Analysis of the Myomegalin Variants by Northern Blot and

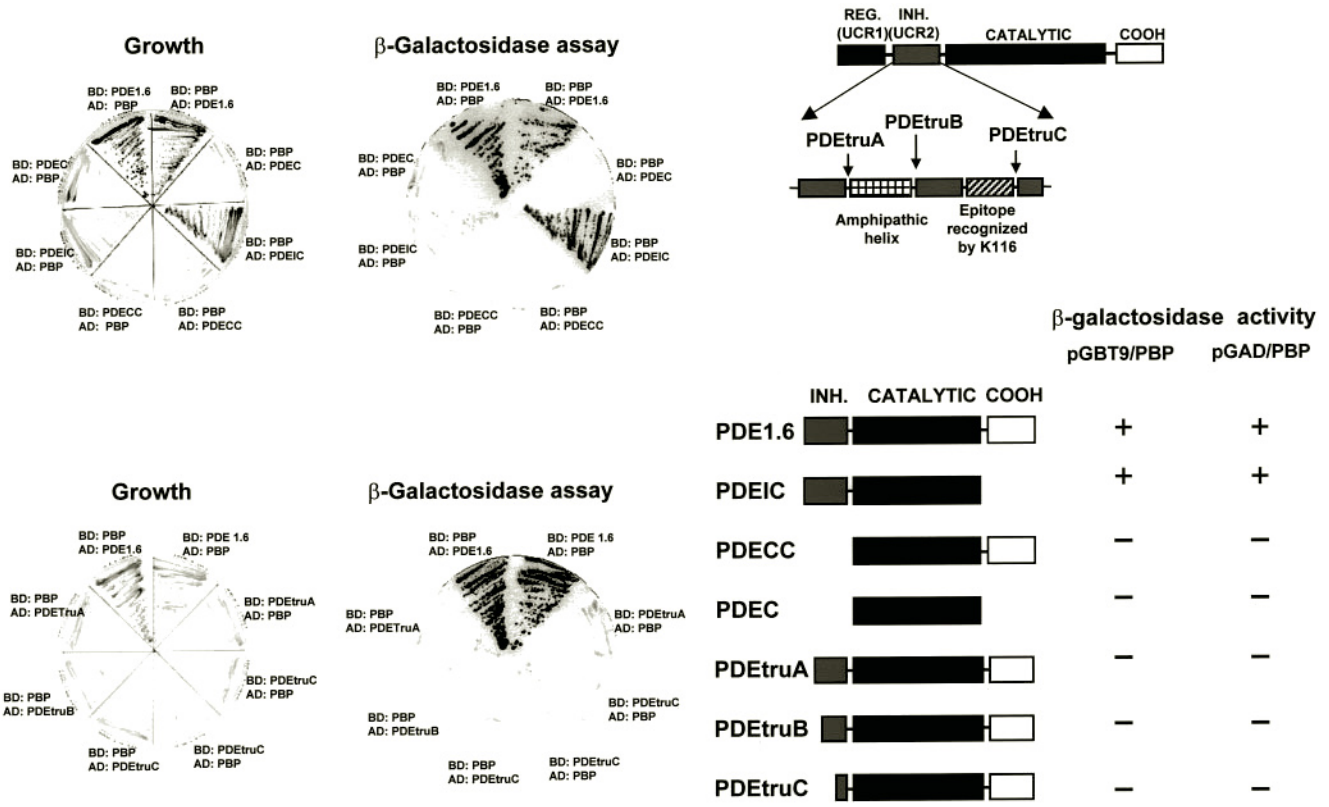

FIG. 1. **Interaction between the carboxyl terminus region of myomegalin and PDE4D using the yeast two-hybrid assay.** The PBP46 construct corresponds to amino acid 1765 to 2324 of myomegalin. The PDE4D construct used (PDE1.6) contains the inhibitory domain, the catalytic domain, and the carboxyl-terminal domain. The PDE constructs with the different deletions and the myomegalin construct (PBP46 cDNA) were subcloned in either pGBT9 in frame with the DNA binding domain (*BD*) or pGAD10 in frame with AD. These different constructs were used for transformation of the yeast Y190 strain using the lithium acetate method (see "Experimental Procedures"). Interaction was assessed by growth in triple dropout medium and by measuring the β-galactosidase activity. A representative experiment of the three performed is reported.

RT-PCR Analysis—To investigate whether different myomegalin transcripts are present in rat and to analyze their tissue distribution, Northern blot analysis was performed using probes corresponding to the 3′ end (probe 1) and 5′ end (probe 2) of the myomegalin ORF (Fig. 3*A*). The results indicated the presence of abundant transcripts of ~7.5–8 kb (myomegalin-1) in heart and skeletal muscle, which contains the entire ORF of myomegalin (Fig. 3*B*). The 7.5–8-kb transcripts were also detected in small amounts in brain, lung, and liver, and hybridized to both probe 1 and probe 2. Probe 1 also detected shorter transcripts, ~5.9 kb in heart and ~2.5 kb in testis, that were not detected with probe 2 (Fig. 3*C*), indicating that these transcripts lack the 5′ end of the coding sequence. The use of probe 2 also revealed the presence of a fourth transcript, ~4.3 kb, present in skeletal muscle (Fig. 3*C*). Thus, there are at least four different transcripts of rat myomegalin: a 7.5-kb transcript expressed in heart and skeletal muscle, a 5.9-kb transcript in heart, a 4.3-kb transcript in skeletal muscle, and one specific for the testis (2.5 kb). The 2.5-kb variant, which is the shortest form, roughly corresponds to the PBP46 clone isolated in the yeast two-hybrid screening and is expressed exclusively in rat testis. The presence of this shorter form was confirmed by the isolation of two cDNA clones from a testis cDNA library (data not shown), even though the initiation methionine of this ORF could not be unequivocally identified. Finally, additional variants at both the 5′ and 3′ ends may be present on the basis of the cDNAs retrieved (data not shown).

A BLAST search of human nucleotide expressed sequence tag sequences indicated a high degree of conservation of rat myomegalin and two overlapping clones identified by sequencing randomly sampled clones with insert sizes of 5–7 kb (KIAA0477 and KIAA0454) from a human brain library (GenBank™ AB007946 and AB007923). The homology encompassed most of the coding sequence except for the 5′ end, again suggesting the presence of splicing in the mRNA. To verify this possibility, RT-PCR analysis was performed with mRNA from rat heart and skeletal muscle. Different primers corresponding to 3′ (MYO3 and MYO4) and 5′ end (MYO1 and MYO2) sequence of myomegalin, and one primer (KIA1) corresponding to the 5′ end of human sequence (Fig. 3*A*) were used for amplification. This analysis indicated that transcripts expressed in the heart and skeletal muscle most likely contain the entire myomegalin ORF defined by cDNA cloning (Fig. 3, *D* and *E*). It also uncovered the presence of an additional transcript containing the 5′ end sequence orthologous to the human clone in heart but not in skeletal muscle. The sequencing of the KIA1-MYO2 PCR fragments from rat heart confirmed the presence of a variant similar to that present in human (data not shown). This amino terminus does not contain a leucine zipper domain.

Expression of the Myomegalin Protein—To investigate the properties of the protein, antibodies were raised against four peptides corresponding to the carboxyl terminus region of myomegalin. Of the different antisera generated, one was further characterized (PBP4). This antibody recognized the tagged 64-kDa myomegalin in the particulate fraction of transfected cells (Fig. 4*A*). This truncated myomegalin form could not be solubilized with nonionic detergent but was partially extracted with RIPA buffer (data not shown).

Western blot analysis with the PBP4 antibody recognized proteins of ~230–250 kDa in heart and skeletal muscle (Fig. 4*B*). Additional immunoreactive bands of ~150 kDa and 115 and 180 kDa were observed in heart and skeletal muscle, respectively. Although a degradation of the 230–250-kDa species cannot be excluded, it is possible that these additional

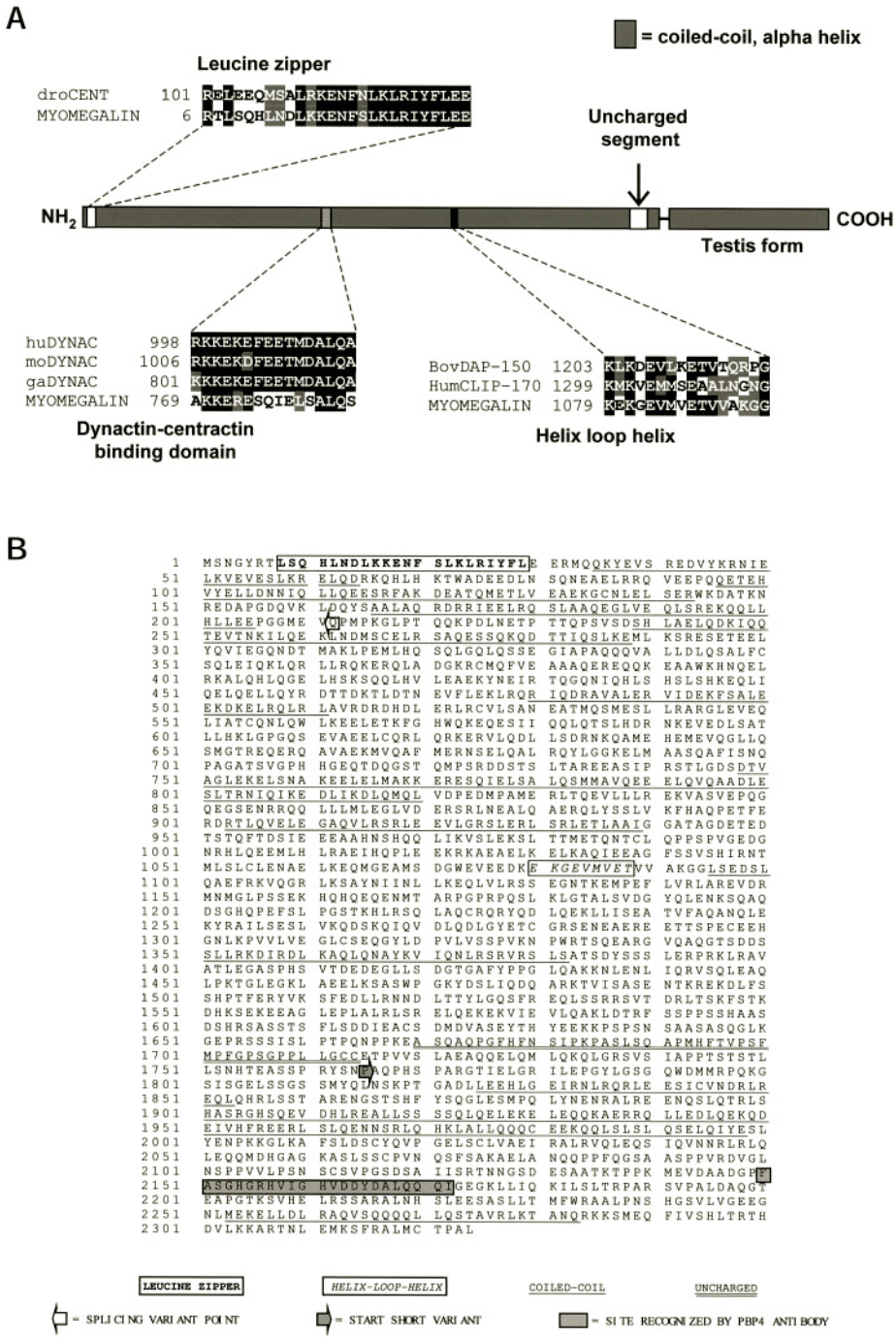

FIG. 2. **Structure of myomegalin.** A diagram of the structure of myomegalin is reported in *panel A*. The regions of homology with the *Drosophila* centrosomin (*droCENT*) dynactin (*HumDYNAC*), bovine DAP-150 (*Bov DAP-150*), and Clip-170 (*HumCLIP-170*) are highlighted together with the alignment of the homologous regions. Identical residues are in *black*, while conservative substitutions are in *gray*. *B*, deduced amino acid sequence of myomegalin. The *gray arrow* in the sequence indicates the beginning of the PBP46 clone. The *gray box* corresponds to the sequence of the peptide used to generate the PBP4 antibody. The coiled-coil regions were identified using the Garnier program. The uncharged domain contains a potential Src homology 3 binding domain.

bands correspond to splicing variants of myomegalin. A 62-kDa protein was consistently observed in rat testis (Fig. 4*C*) or germ cell extracts (data not shown). These proteins were completely insoluble in standard homogenization conditions and could be partially solubilized from muscle only under conditions that extract the myofibril components (Fig. 4).

Localization of Myomegalin in Cultured Cells—Because of the tight binding of myomegalin to particulate structures, immunocytochemistry was used to further analyze the localization of this protein in transfected COS-7 cells. The truncated form of myomegalin (PBP46; aa 1765–2324) fused to a flag epitope was transfected in COS-7 cells and the distribution detected with a myomegalin-specific antibody (PBP4), and with an anti-flag antibody (Fig. 5*A*). An overlapping pattern of immunofluorescence was obtained with both antibodies confirming the specificity of the PBP4 antiserum for immunofluorescence localization. Moreover, a signal with PBP4 was found in cells negative for the flag antibody, indicating the presence of endogenous myomegalin in COS-7 cells. This expression in COS-7 cells was confirmed by detection of myomegalin transcripts by PCR amplification (data not shown). The endogenous myomegalin localized in an inner Golgi/centrosome region that corresponds to the location of the transfected myomegalin. To further define the site of myomegalin localization in these cells, centrosomal and Golgi markers were used to demonstrate an overlapping localization with the two markers (Fig. 5, *B* and *C*). Similar localization of myomegalin was also observed in cultured FRTL-5 thyroid cells (data not shown). In these latter cells, PDE4D is localized predominantly in a similar Golgi/centrosomal region (16).

Colocalization of Myomegalin and PDE4D in Muscle Cells and Testis—Because myomegalin transcripts are highly ex-

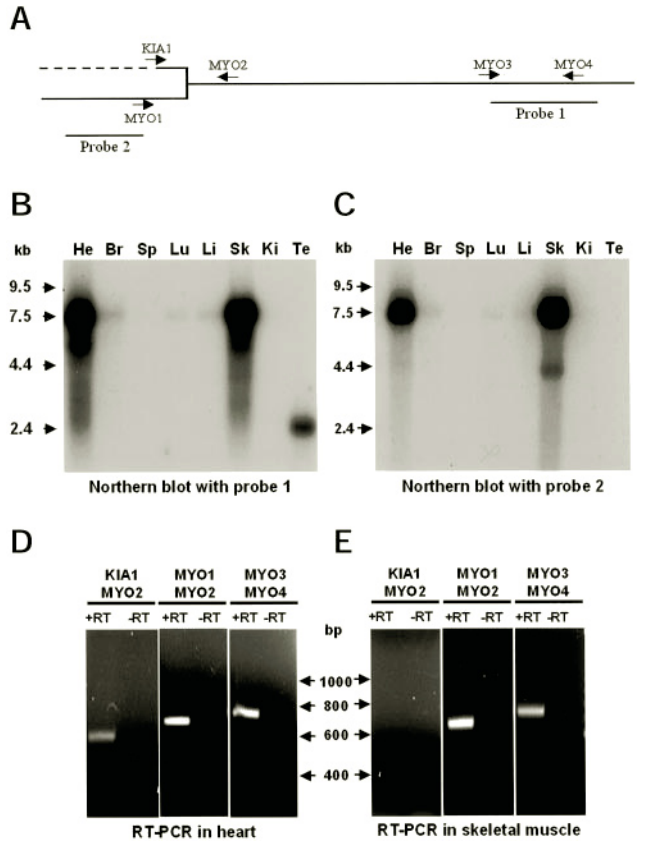

FIG. 3. **Identification of the different myomegalin variants and their tissue distribution.** *A*, schematic representation of the splicing boundary in the myomegalin sequence, the probes used for Northern blot analysis, and the PCR primers used. *B* and *C*, Northern blot analysis of different rat tissues using probes at the 3′ end (probe 1) and the 5′ end (probe 2) of myomegalin mRNA. *He*, heart; *Br*, brain; *Sp*, spleen; *Lu*, lung; *Li*, liver; *Sk*, skeletal muscle; *Ki*, kidney; *Te*, testis. Exposure time was 17–20 h. *D* and *E*, RT-PCR analysis of the expression of the two long variants of myomegalin. RT-PCR was performed with the pair of primers reported above the lanes. In some reactions, the reverse transcriptase was omitted as a negative control (*−RT*). The identity of the products was confirmed by sequencing.

pressed in heart and skeletal muscle, myomegalin and PDE4D localization was assessed in sections of cardiac (not shown) and skeletal muscle (Fig. 6). Staining with the PBP4 antibody yielded a periodic pattern (~2 μm) of myomegalin localization along muscle fibrils in skeletal (Fig. 6) and cardiac (data not shown) tissues. Double staining using a myomegalin-specific antibody (PBP4) and a PDE4D-specific antibody (M3S1) indicated colocalization of both proteins in the same region of the myofibers (Fig. 6). This region corresponds to the z band on the basis of a comparison with the staining of the fibers with myosin, actin, and desmin antibodies (data not shown).

In testis, myomegalin immunoreactivity was mostly present in germ cells of the seminiferous tubules. The antibody stained a region in close proximity to the nucleus, corresponding to the Golgi complex of pachytene spermatocytes and round spermatids (Fig. 7). This predominant expression of the short myomegalin variant in germ cells was confirmed by PCR analysis, Northern blot, and Western blot of extracts from either seminiferous tubules or isolated germ cells (data not shown).

Myomegalin and PDE4D3 Subcellular Localization in the Intact Cell—Solubilization of the full-length myomegalin could not be achieved under nondenaturing conditions. However, the truncated myomegalin (PBP46), even though particulate after overexpression, could be partially solubilized with RIPA buffer containing 0.1% SDS. To determine whether this myomegalin variant interacts with PDE4D, expression vectors for PDE4D3 and the truncated myomegalin (PBP46) were cotransfected in COS-7 cells. Cells were solubilized with RIPA and the extract subjected to immunoprecipitation with PDE4D-selective antibodies. Under these conditions, the PDE4D-selective antibody coimmunoprecipitated the truncated myomegalin in complex with the PDE (Fig. 8*B*). The immunoprecipitation was specific because, in the absence of PDE4D3, no myomegalin was recovered in the immunoprecipitate even after overexposure of the film (data not shown). Moreover, no myomegalin or PDE was immunoprecipitated when unrelated IgG was used in this assay (data not shown). Myomegalin was recovered in the immunoprecipitation pellet when PDE4D1 and PDE4D3 were used for transfection, but not with the PDE4D2 variant, which lacks the putative domain interacting with myomegalin (Fig. 8*C*). This latter finding indicates that not all PDE variants interact with this myomegalin form.

To further confirm the interaction between the two proteins in intact cells, expression vectors for PDE4D3 and PBP46 were cotransfected in COS-7 cells. After 24 h the cells were homogenized, the particulate fraction separated by centrifugation, and the PDE activity recovered in this fraction of the homogenate was measured. Cotransfection of PDE4D3 and PBP46 led to a 2–4-fold increase in the PDE activity recovered in the particulate fraction (Fig. 9*A*) as compared with the cells transfected with PDE4D3 alone. Western blot analysis with PDE4D-specific antibodies confirmed the PDE activity data. Although the 93-kDa PDE4D3 was at the limit of detection in the particulate fraction of COS-7 cells transfected only with PDE4D3, cotransfection with myomegalin produced an increase in the PDE4D3 protein recovered in the particulate fraction (Fig. 9*B*). In agreement with previous observations, the short myomegalin variant was recovered almost exclusively in the particulate fraction of COS-7 cells (Fig. 9*C*).

DISCUSSION

With these studies, we report the identification and the initial characterization of myomegalin, a novel protein with the properties of a structural/scaffold protein. At least three potential splicing variants of myomegalin detected in rat may serve distinct functions in muscle and nonmuscle cells. Myomegalin is targeted to the Golgi/centrosomal region in cultured COS-7 and FRTL-5 cells and in germ cells of the testis, whereas in cardiac and skeletal muscle it is associated with the sarcomere or the sarcoplasmic reticulum. We propose that one of the functions of this protein is in cAMP signaling compartmentalization because it targets a PDE component of the cAMP signaling to these subcellular structures.

Myomegalin is structurally related to the *Drosophila* centrosomin (*cnn*). Centrosomin was originally identified while screening for genes regulated by antennapedia or other homeotic genes (26) and is mostly composed of coiled-coil structures with three leucine zipper domains. The first leucine zipper near the amino terminus is very similar to the only leucine zipper found in one variant of myomegalin. The extensive arrangement in coiled-coil structures is also shared between centrosomin and myomegalin. The *Drosophila* centrosomin is a component of the centrosomes and the mitotic spindle (30) and is thought to play a crucial role during morphogenesis of the central nervous system and midgut (26). A testis-specific isoform of centrosomin has been described in fly (31). Mutations that disrupt the spermatogenic-specific centrosomin impair cytokinesis, kariokinesis, and organization of the sperm axoneme. In a strikingly similar fashion, a splicing variant of the mammalian myomegalin is expressed in germ cells of rat testis and is localized in a Golgi/centrosomal region of pachytene spermatocytes and round spermatids; however, it could not conclusively be determined whether it is located in the basal

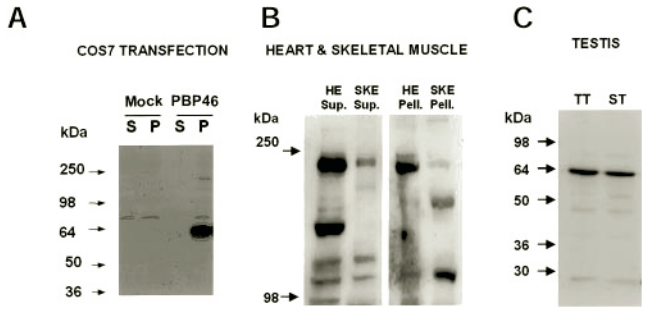

FIG. 4. **Western blot analysis of myomegalin expression using the PBP4 antibody.** *A*, COS-7 cells were transfected with a pCEPflag-PBP46 construct or with empty vector (mock). After 24 h, cells were harvested in homogenization buffer and the extract centrifuged at 14,000 × *g* for 30 min. Pellets (*P*) and supernatant (*S*) were fractionated on SDS-PAGE, and the migration of the recombinant myomegalin was monitored using anti-flag antibodies. *B*, rat heart and skeletal muscle tissue was homogenized according to the procedure detailed under "Experimental Procedures." Pellets and supernatants were fractionated on SDS-PAGE. After transfer, membranes were probed with the PBP4 antibody. *C*, total testis (*TT*) or seminiferous tubules (*ST*) were homogenized and aliquots of the homogenates fractionated on SDS-PAGE. After transfer, the membrane was probed with the PBP4 antibody.

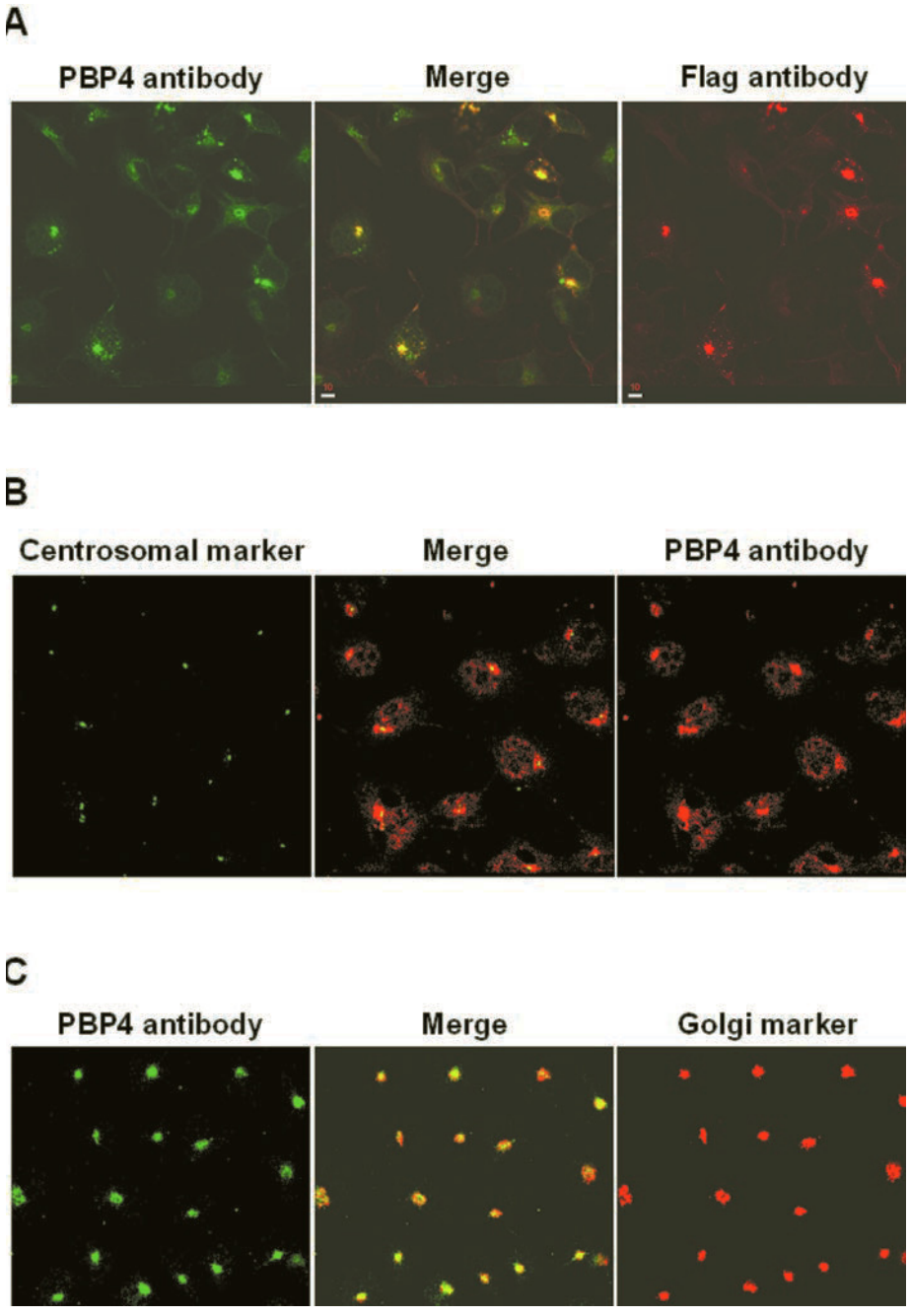

FIG. 5. **Subcellular localization of endogenous and recombinant myomegalin in COS-7 cells.** *A*, COS-7 cells were transfected with the pCEPflag-PBP46 construct. Twenty-four h after transfection, cells were stained with the myomegalin-specific antibodies (PBP4) or with the flag epitope antibodies. Fluorescein isothiocyanate-conjugated anti-rabbit secondary antibodies (*green*) and rhodamine-conjugated anti-mouse IgG secondary antibodies (*red*) were used to detect the PBP4 and the monoclonal flag antibody, respectively. Pictures were captured with a confocal microscope and merged. *B*, immunofluorescence staining of untransfected COS-7 cells with the centrosomal marker CTR453 and with PBP4 antibody. *C*, immunofluorescence staining of untransfected COS-7 cells with the PBP4 antibody and with the Golgi marker CTR433.

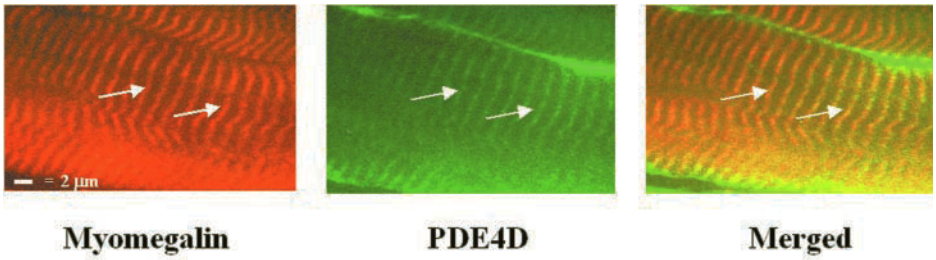

FIG. 6. **Colocalization of myomegalin and PDE4D in mouse skeletal muscle.** Sections of mouse skeletal muscle were stained with myomegalin (PBP4, *red*) and PDE4D-specific (M3S1, *green*) antibodies. The distance between the two contiguous bands was estimated to be 2 μm, consistent with the length of a sarcomere. The staining with myomegalin and PDE4D antibodies overlapped with that of desmin but not with either myosin or actin. The periodic pattern of PDE4D staining was confirmed by a second polyclonal anti-PDE4 antibody. In all instances, staining could be blocked by preadsorption of the primary antibody with the corresponding peptide or fusion protein. Similar results were obtained with rat skeletal muscle.

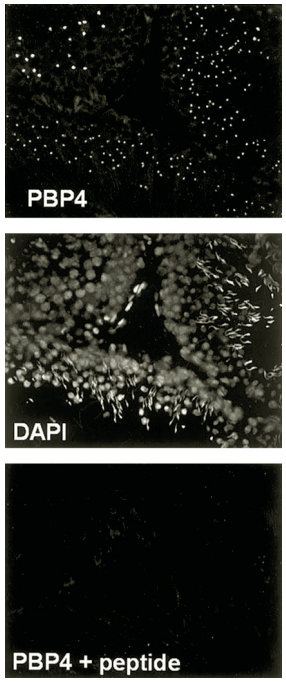

FIG. 7. **Cellular localization of testis-specific myomegalin in germ cells.** Sections of adult rat testis were stained with the myomegalin antibody (PBP4) in the absence or presence of peptide PBP4. DAPI was used to stain the nuclei of developing germ cells and somatic cells.

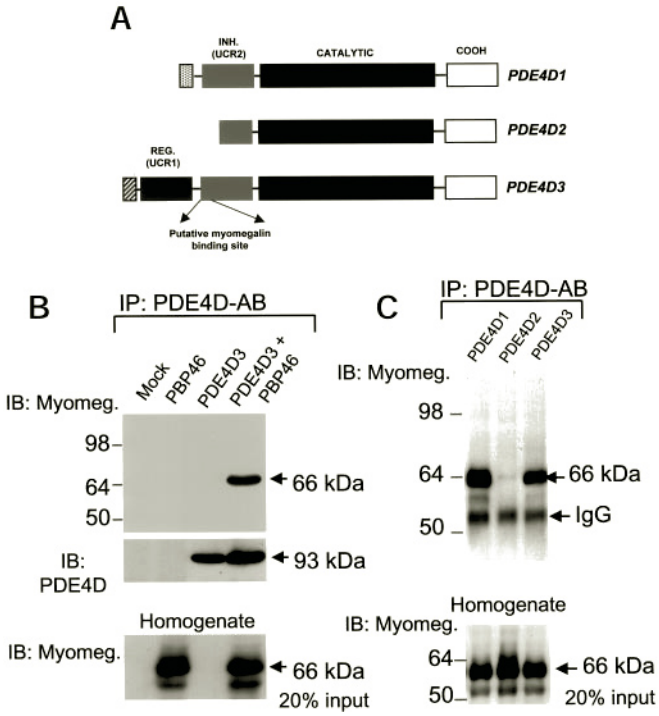

FIG. 8. **Coimmunoprecipitation of myomegalin and PDE4D3.** *A*, diagram of the domains present in the three PDE4D variants used for the coimmunoprecipitation. *B*, COS cells were transfected with either a PDE4D (pCMV5-PDE4D3) or a myomegalin (pCEP4-PBP46) expression vector or a combination of the two. After homogenization and centrifugation, the supernatant and the RIPA-extracted supernatant were combined and subjected to immunoprecipitation with PDE4D-selective monoclonal antibodies. The pellets of the immunoprecipitation or an aliquot of the supernatant before precipitation were analyzed by SDS-PAGE and Western blot using either myomegalin- (PBP4) or PDE4D-selective (M3S1) antibodies. When immunoprecipitation was carried out with nonimmune IgG as a control, neither PDE4D3 nor myomegalin were recovered in the pellet (data not shown). *C*, COS cells were cotransfected with vectors containing PDE4D1, PDE4D2, or PDE4D3 cDNAs and a myomegalin expression plasmid (pCEP4-PBP46). After 24 h, cell extracts were prepared and processed for immunoprecipitation and Western blot analyses as reported for *panel B*.

body of the developing flagellum. Thus, it is likely that the mammalian myomegalin has functions during spermatogenesis that overlap with those of the centrosomin in *Drosophila*.

It should be pointed out that other mammalian proteins homologous to the *Drosophila* centrosomin have been described previously. These include mouse centrosomin A and B and human 167 protein (32–34). However, their similarity to the *Drosophila* centrosomin protein is low, and myomegalin is more related to centrosomin than to these mammalian centrosomins. The function of mammalian centrosomin is at present unknown.

Recently, several large coiled-coil proteins localized in the Golgi apparatus have been classified as a distinct golgin family of proteins (35–37). Among the many members identified, golgin-230/245/256, golgin 97, GM130, and giantin proteins have extensive coiled-coil structure and a domain at the carboxyl terminus that specifies Golgi targeting (grip domain). Myomegalin is weakly homologous to golgin 230/245/256 (20% identity, 40% conservative substitutions) in several coiled-coil domains. However, a domain similar to the grip domain could not be identified at the carboxyl terminus of myomegalin, even though the last 550 amino acids of this latter protein are sufficient to target it to the Golgi/centrosome structures.

Although formal proof of an interaction of PDE4D with the full-length myomegalin was precluded by the insolubility of the protein, we have provided evidence of an interaction of the 62–64-kDa myomegalin variant with PDE4D. Four independent lines of evidence indicate that the two proteins may indeed exist in a complex in the intact cell. In addition to the interaction detected with the yeast two-hybrid screening, the 64-kDa variant of myomegalin and PDE4D interact specifically in a coimmunoprecipitation assay. Furthermore, cotransfection of

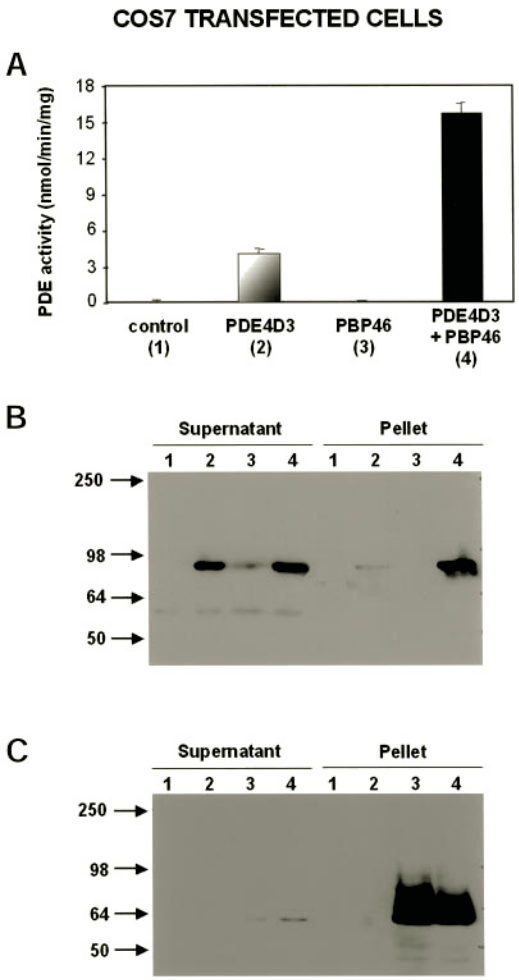

FIG. 9. **Recovery of PDE4D3 in the insoluble fraction after cotransfection with myomegalin.** COS-7 cells were transfected with plasmids pCDNA3-PDE4D3, pCEP4-PBP46 alone, or in combination. Mock-transfected cells received an empty vector only. After 24 h, cells were harvested, homogenized, and the soluble and particulate fractions were isolated by centrifugation at 14000 $\times$ *g* for 30 min. Pellets were washed twice and resuspended in the same buffer. An aliquot of the pellet was used for the PDE assay (*A*). Aliquots of the pellet and supernatants were fractionated by SDS-PAGE, blotted, and probed with PDE4D-specific antibodies (M3S1) (*B*) or with anti-flag antibodies (*C*). Comparable amounts of soluble and particulate proteins were loaded in each lane. Protein content was determined by the Bradford method. A representative experiment of the three performed is reported.

myomegalin targeted the recombinant PDE4D3 to the particulate fraction of COS-7 cells. Finally, myomegalin and PDE4D were colocalized in cultured cells as well as in cardiac and skeletal muscle tissue.

Deletion mutagenesis of PDE4D indicates that a site of interaction with myomegalin is in a domain that corresponds to the amino terminus of the upstream conserved region 2 (UCR2). This domain is conserved in all the long forms of PDE4 opening the possibility that other PDE4s may interact with myomegalin. This interacting domain of PDE4D consists of a region of predicted α-helical structure with amphipathic distribution of the charges. The carboxyl terminus of myomegalin also contains α-helical domains that may mediate the interaction with a PDE. Using the yeast two-hybrid assay, we have reported that this PDE4D domain, which interacts with myomegalin, is also involved in intramolecular interactions with the amino-terminal regulatory domain and that it functions as an autoinhibitory domain that modulates the catalytic activity of the enzyme (18). At present, it is not clear whether the intramolecular interaction and the binding to myomegalin are mutually exclusive or if they can occur at the same time, nor is it known whether the binding of myomegalin alters the catalytic activity of the PDE. We have reported that phosphorylation of PDE4D3 alters the interaction of this domain with the amino terminus (18); it is then possible that the state of phosphorylation also affects the ability of the PDE4D to interact with myomegalin. Further studies are required to clarify this issue. It is possible that the interaction of PDE4D with myomegalin, and therefore with the Golgi/centrosome, may be a dynamic process and that translocation of this protein may occur during signaling. Indeed, data have recently been reported indicating that PDE4D3 may translocate upon activation of the mitogen-activated protein kinase pathway (38).

In view of its extensive coiled-coil composition, it is likely that myomegalin either oligomerizes with itself or interacts with other proteins. The presence of a leucine zipper domain, which is also known to mediate protein/protein interaction, is consistent with this conclusion. In addition to a PDE, other proteins may be interacting with myomegalin. Using homology searches, a domain similar to the domain involved in dynactin-centractin interaction, a helix-loop-helix found in Clip170, and an uncharged domain that resembles an Src homology 3 binding domain, were identified. Thus, the presence of these putative interacting domains suggests that myomegalin is present in a complex with several additional proteins, which may be involved in vesicle transport or with their interaction with cytoskeletal structures. This raises the possibility that myomegalin may play a role in vesicle transport between the different layers of the Golgi stack.

Myomegalin is expressed at high levels in skeletal and cardiac tissue, suggesting an important function in muscle cells. Upon staining with a myomegalin antibody, a periodic pattern was observed indicating localization either in the z region between sarcomeres or in the sarcoplasmic reticulum. It could not be determined whether PDE4D and myomegalin are in the z band proper or are associated with the sarcoplasmic reticulum. Several other cAMP-signal transduction proteins have been localized in the same region of the sarcomere including adenylyl cyclase, L channels, and the regulatory subunit of PKA (39, 40). Thus, it is plausible that myomegalin brings PDE4D to a site where several steps in the cAMP signaling cascade take place in muscle cells.

The colocalization of PDE4D and myomegalin in Golgi/centrosomal structures points to a role of cyclic nucleotide signaling in the function of these organelles. Targeting of a PDE to the Golgi may have an important function in controlling cAMP diffusion to these regions. Interestingly, PKA regulatory subunits, and anchoring AKAPs, have also been localized in the Golgi apparatus and in the centrosome (8, 9, 41, 42). Thus, our findings suggest that PDE4D localization in these regions serves to control the state of activation of PKAs and therefore the cAMP-regulated phosphorylations in these domains. The exact role of cAMP signaling in centrosome function and in vesicle transport in the Golgi is largely unknown, even though there is ample indirect evidence that cAMP regulates both cytoskeleton assembly as well as vesicle transport (43, 44). Pigment granule redistribution in *Xenopus* melanocytes is regulated by cAMP (45), and cyclic nucleotides have long been implicated in the control of flagellar movements (46). Thus, it is possible that strategic localization of a PDE in these regions via myomegalin interaction may be involved in the control of organelle movements or cytoskeletal assembly/disassembly.

Acknowledgments—We acknowledge Dr. Michel Bornens for constructive comments and for the gift of the centrosomal and Golgi anti-

bodies, and Dr. Kjetil Tasken for helpful discussions and advice with these studies.

REFERENCES

1. Cohen, G. B., Ren, R., and Baltimore, D. (1995) *Cell* **80,** 237–248
2. Mochly-Rosen, D. (1995) *Science* **268,** 247–251
3. Rubin, C. S. (1994) *Biochim. Biophys. Acta* **1224,** 467–479
4. Colledge, M., and Scott, J. D. (1999) *Trends Cell Biol.* **9,** 216–221
5. Coghlan, V. M., Perrino, B. A., Howard, M., Langeberg, L. K., Hicks, J. B., Gallatin, W. M., and Scott, J. D. (1995) *Science* **267,** 108–111
6. Rosenmund, C., Carr, D. W., Bergeson, S. E., Nilaver, G., Scott, J. D., and Westbrook, G. L. (1994) *Nature* **368,** 853–856
7. Johnson, B. D., Scheuer, T., and Catterall, W. A. (1994) *Proc. Natl. Acad. Sci. U. S. A.* **91,** 11492–11496
8. Nigg, E. A., Hilz, H., Eppenberger, H. M., and Dutly, F. (1985) *EMBO J.* **4,** 2801–2806
9. De Camilli, P., Moretti, M., Donini, S. D., Walter, U., and Lohmann, S. M. (1986) *J. Cell Biol.* **103,** 189–203
10. Beavo, J. A. (1995) *Physiol. Rev.* **75,** 725–748
11. Conti, M., and Jin, S.-L. C. (1999) *Prog. Nucleic Acids Res. Mol. Biol.* **63,** 1–38
12. Conti, M., Nemoz, G., Sette, C., and Vicini, E. (1995) *Endocr. Rev.* **16,** 370–389
13. Houslay, M. D., Sullivan, M., and Bolger, G. B. (1998) *Adv. Pharmacol.* **44,** 225–342
14. Bolger, G. B., Erdogan, S., Jones, R. E., Loughney, K., Scotland, G., Hoffmann, R., Wilkinson, I., Farrell, C., and Houslay, M. D. (1997) *Biochem. J.* **328,** 539–548
15. Iona, S., Cuomo, M., Bushnik, T., Naro, F., Sette, C., Hess, M., Shelton, E. R., and Conti, M. (1998) *Mol. Pharmacol.* **53,** 23–32
16. Jin, S. L., Bushnik, T., Lan, L., and Conti, M. (1998) *J. Biol. Chem.* **273,** 19672–19678
17. Pryzwansky, K. B., Kidao, S., and Merricks, E. P. (1998) *Cell Biochem. Biophys.* **28,** 251–275
18. Lim, J., Pahlke, G., and Conti, M. (1999) *J. Biol. Chem.* **274,** 19677–19685
19. Graham, F. L., and van der Eb, A. J. (1973) *Virology* **52,** 456–467
20. Brandt, P. W., Diamond, M. S., Rutchik, J. S., and Schachat, F. H. (1987) *J. Mol. Biol.* **195,** 885–896
21. Jasmin, B. J., Cartaud, J., Bornens, M., and Changeux, J. P. (1989) *Proc. Natl. Acad. Sci. U. S. A.* **86,** 7218–7222
22. Bailly, E., Doree, M., Nurse, P., and Bornens, M. (1989) *EMBO J.* **8,** 3985–3995
23. Salanova, M., Chun, S. Y., Iona, S., Puri, C., Stefanini, M., and Conti, M. (1999) *Endocrinology* **140,** 2297–2306
24. Thompson, W. J., and Appleman, M. M. (1971) *Biochemistry* **10,** 311–316
25. Bradford, M. M. (1976) *Anal. Biochem.* **72,** 248–254
26. Heuer, J. G., Li, K., and Kaufman, T. C. (1995) *Development* **121,** 3861–3876
27. Burkhardt, J. K. (1998) *Biochim. Biophys. Acta* **1404,** 113–126
28. Pierre, P., Scheel, J., Rickard, J. E., and Kreis, T. E. (1992) *Cell* **70,** 887–900
29. Holzbaur, E. L., Hammarback, J. A., Paschal, B. M., Kravit, N. G., Pfister, K. K., and Vallee, R. B. (1991) *Nature* **351,** 579–583
30. Megraw, T. L., Li, K., Kao, L. R., and Kaufman, T. C. (1999) *Development* **126,** 2829–2839
31. Li, K., Xu, E. Y., Cecil, J. K., Turner, F. R., Megraw, T. L., and Kaufman, T. C. (1998) *J. Cell Biol.* **141,** 455–467
32. Joswig, G., Petzelt, C., and Werner, D. (1991) *J. Cell Sci.* **98,** 37–43
33. Petzelt, C., Joswig, G., Mincheva, A., Lichter, P., Stammer, H., and Werner, D. (1997) *J. Cell Sci.* **110,** 2573–2578
34. Scholler, J. K., and Kanner, S. B. (1997) *DNA Cell Biol.* **16,** 515–531
35. Munro, S., and Nichols, B. J. (1999) *Curr. Biol.* **9,** 377–380
36. Barr, F. A. (1999) *Curr. Biol.* **9,** 381–384
37. Kjer-Nielsen, L., Teasdale, R. D., van Vliet, C., and Gleeson, P. A. (1999) *Curr. Biol.* **9,** 385–388
38. Liu, H., and Maurice, D. H. (1999) *J. Biol. Chem.* **274,** 10557–10565
39. Gao, T., Puri, T. S., Gerhardstein, B. L., Chien, A. J., Green, R. D., and Hosey, M. M. (1997) *J. Biol. Chem.* **272,** 19401–19407
40. Yang, J., Drazba, J. A., Ferguson, D. G., and Bond, M. (1998) *J. Cell Biol.* **142,** 511–522
41. Keryer, G., Rios, R. M., Landmark, B. F., Skalhegg, B., Lohmann, S. M., and Bornens, M. (1993) *Exp. Cell Res.* **204,** 230–240
42. Witczak, O., Skalhegg, B. S., Keryer, G., Bornens, M., Tasken, K., Jahnsen, T., and Orstavik, S. (1999) *EMBO J.* **18,** 1858–1868
43. Jilling, T., and Kirk, K. L. (1996) *J. Biol. Chem.* **271,** 4381–4387
44. Muniz, M., Martin, M. E., Hidalgo, J., and Velasco, A. (1997) *Proc. Natl. Acad. Sci. U. S. A.* **94,** 14461–14466
45. Reilein, A. R., Tint, I. S., Peunova, N. I., Enikolopov, G. N., and Gelfand, V. I. (1998) *J. Cell Biol.* **142,** 803–813
46. Bloodgood, R. A. (1992) *Biol. Cell* **76,** 291–301
47. Gietz, D., St. Jean, A., Woods, R. A., and Schiestl, R. H. (1992) *Nucleic Acids Res.* **20,** 1425